6

Theory and Design of Micromechanical Vibratory Gyroscopes

Vladislav Apostolyuk

1. INTRODUCTION

Fabrication technologies for microcomponents, microsensors, micromachines and microelectromechanical systems (MEMS) are being rapidly developed, and represent a major research effort worldwide. There are many techniques currently being utilised in production of different types of MEMS, including inertial microsensors, which have made it possible to fabricate MEMS in high volumes at low individual cost. Micromechanical vibratory gyroscopes or angular rate sensors have a large potential for different types of applications as primary information sensors for guidance, control and navigation systems. They represent an important inertial technology because other gyroscopes such as solid-state gyroscopes, laser ring gyroscopes and fibre optic gyroscopes, do not allow for significant miniaturisation. MEMS sensors are commonly accepted as low performance and low cost sensors. Nevertheless, recent applications have resulted in the need for sensors with improved performances. High performances could be achieved by means of improved sensitive element and circuit design.

One of the ways to improve performances of micromechanical vibratory gyroscopes is to analyze their dynamics and errors in order to find efficient design methodologies. Some mathematical models of symmetrical (without decoupling frames) sensitive elements with translation movement of a proof mass, applicable to analysis of micromechanical gyroscopes as well as control principles were considered in [1, 2]. Dynamics and errors of micromechanical gyroscopes with decoupling frame were studied in [3–5]. Generalised analytical approaches to design were presented in [6], which allow avoiding numerous

simulations and experimental researches to try to find appropriate designs for sensitive elements.

Here we are going to study a general approach to the analysis of the dynamics and errors of different types of micromechanical vibratory gyroscopes as well as calculation of their performances for application in the design of such gyroscopes.

2. OPERATION PRINCIPLE AND CLASSIFICATION

In most micromechanical vibratory gyroscopes, the sensitive element can be represented as an inertia element and elastic suspension with two prevalent degrees of freedom (see figure 1). Massive inertia element is often called proof mass. The sensitive element is driven to oscillate at one of its modes with prescribed amplitude. This mode usually is called primary mode. When the sensitive element rotates about a particular fixed-body axis, which is called sensitive axis, the resulting Coriolis force causes the proof mass to move in a different mode. Contrary to the classical angular rate sensors based on the electromechanical gyroscopes, information about external angular rate is contained in these different oscillations rather than non-harmonic linear or angular displacements. Hereafter, excited oscillations are referred to as primary oscillations and oscillations caused by angular rate are referred to as secondary oscillations or secondary mode.

In general, it is possible to design gyroscopes with different types of primary and secondary oscillations. For example, a combination of translation as primary oscillations and rotation as secondary oscillations as was implemented in a so-called tuning-fork gyroscope. It is worth mentioning that the nature of the primary motion does not necessarily have to be oscillatory but could be rotary as well. Such gyroscopes are called rotary vibratory gyroscopes. However, it is typically more convenient for the vibratory gyroscopes to be implemented with the same type and nature of primary and secondary oscillations.

With respect to the number of inertia elements used, the nature of primary and secondary motions of the sensitive element, classification of the vibratory gyroscopes can be

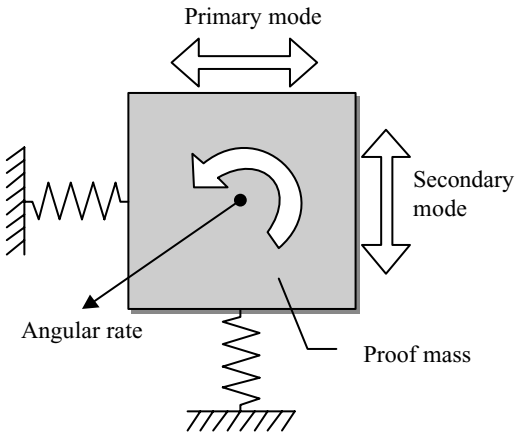

FIGURE 1. Operation principle.

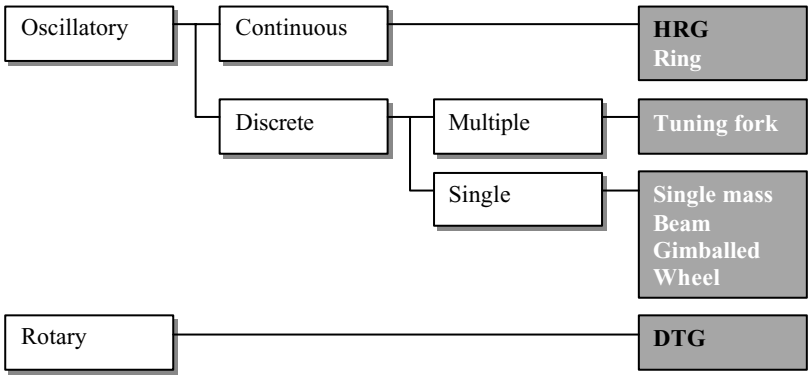

FIGURE 2. Classification of the vibratory gyroscopes.

represented as shown in the figure 2. Designs that were used to produce micromechanical gyroscopes are shown in white colour.

Top-level separation is done based on the nature of the primary motion. It can be either oscillatory or rotary. Classical dynamically tuned gyroscope (DTG) is an example of the rotary vibratory gyroscope.

Next step involves consideration of the general design of the sensitive element and its mathematical representation. In particular, design of the vibratory sensitive element can be based on continuous vibrating media or discrete (single or multiple) vibrating masses. Corresponding mathematical models are based either on partial differential equations, namely modified wave equation, or systems of ordinary differential equations.

One of the most well known examples of the oscillatory gyroscope with continuous vibrating media is a hemispherical resonating gyroscope (HRG). HRG sensitive element design usually is based on the resonating shell that has a hemispheric or so-called "wine-glass" shape. Primary oscillations are provided by standing wave excited in the rim of the shell. In case of no external angular rate, nodes of the wave do not move. If the sensitive element rotates around sensitive axis, which is orthogonal to the plane of the wave, the secondary oscillations can be detected at the nodes. Despite HRG itself has never been referred to as a micromechanical gyroscope, its operation principle has been widely used in the number of micromechanical designs. In particular, the hemispherical shape of the shell has been replaced with a thin cylinder or a ring.

Because of quite strict limitations to the complexity of mechanical structures that can be produced using micromachining processes, majority of the modern designs of micromechanical gyroscopes make use of a simple structure that consists of a single or multiple massive elements connected to the base by means of elastic suspension. The main purpose of the elastic suspension is to provide proof masses with at least two orthogonal degrees of freedom allowing primary and secondary oscillations. Another task, which is usually assigned to the design of elastic suspension, is to provide sufficient mechanical decoupling between primary and secondary oscillations, thus reducing so-called quadrature errors.

There are few examples of such single discrete mass gyroscope designs. The first is a simple beam or mushroom like structure attached to the base that can deflect in two orthogonal directions. Despite the beam itself has all features of a continuous media vibratory

sensor, its dynamics and operation as an angular rate sensor is sufficiently well described in terms of ordinary differential equations. Therefore this design has been placed in the discrete brunch of the classification rather than distributed.

Another example and one of the most widespread designs is a simple single mass with two-degrees of freedom either with additional decoupling frame or without it, which uses translational primary and secondary oscillations for sensing. In this case elastic suspension consists of set of simple flexible beam-like springs. If translational springs are replaced with rotational ones providing the sensitive element with two rotational degrees of freedom, such a design usually is referred to as a gimballed micromechanical gyroscope. Finally, the wheeled micromechanical gyroscope consists of an oscillating disc that has three rotational degrees of freedom (one for primary mode and two for secondary modes) and as a result can sense two component of the external angular rate.

The difference between most of all modern single-mass micromechanical gyroscopes lays mainly in designs of the mass itself and the elastic suspensions rather than operation principle and its mathematical model. Needless to say that such difference are driven almost solely by specific features of chosen micro-fabrication process. Therefore, mathematical models and design methodologies that are presented here can be directly applied to the analysis of all single mass micromechanical vibratory gyroscopes. In case of continuous media sensors the results still can be applied to some certain extent provided lumped mass mathematical representation is used.

Motion Equations

Initial and the most important step in mathematical model development is deriving of the motion equations. In our case these will be motion equations of the sensitive element of the single mass vibratory gyroscope. One of the most easily formalised approaches is the Lagrange equation:

$$\frac{d}{dt}\left(\frac{\partial L}{\partial \dot{x}_i}\right) - \frac{\partial L}{\partial x_i} = Q_i. \tag{1}$$

Here $L = E_K - E_P$ is the Lagrange's function, E_K and E_P are kinetic and potential energies of the sensitive element respectively, Q_i are generalised forces acting on the sensitive element, and i ranges from 1 to the number of degrees of freedom under consideration. So to make use of the Lagrange equation we need expressions for the kinetic and potential energies of the sensitive element.

First let us have a look at kinematical representation of the sensitive element, which is shown in the figure 3. It consists of a proof mass (m_2), a decoupling frame (m_1), and two sets of generalised springs connecting masses to each other and to the base. Let us introduce the right-handed orthogonal and normalized reference frame $OX_1X_2X_3$ in which primary oscillations are excited along the first axis X_1, secondary oscillations occur along the second axis X_2 and, therefore, the third axis X_3 is the sensitive axis. As a generalized coordinate x_1 (primary oscillations) let us assume displacements of the sensitive element along the axis X_1. Similarly generalized coordinate x_2 corresponds to the displacements of the sensitive element along the axis X_2. Here and after subscribe index number refers to the number of the corresponding axis. Base, in which sensitive element is installed, is assumed

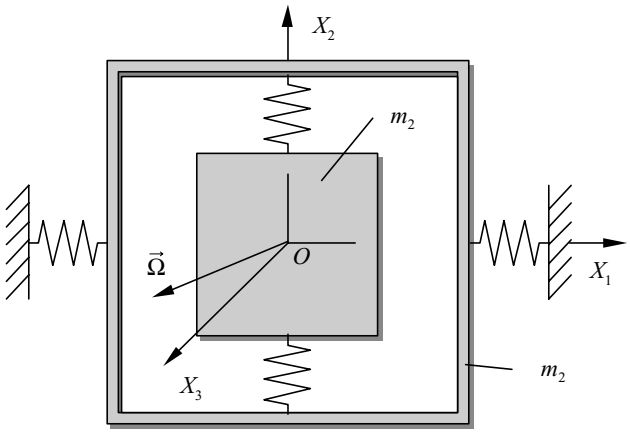

FIGURE 3. Sensitive element of a micromechanical vibratory gyroscope.

to rotate with the arbitrary angular rate $\vec{\Omega}$ that is defined by its projections on the introduced above reference frame as $\vec{\Omega} = \{\Omega_1, \Omega_2, \Omega_3\}$.

First we shall consider sensitive element with translational both primary and secondary motion. The total kinetic energy of the sensitive element in this case will be

$$E_K = \frac{m_2}{2}\left[(\dot{x}_1 - x_2\boldsymbol{\Omega}_3)^2 + (\dot{x}_2 + x_1\boldsymbol{\Omega}_3)^2 + (x_2\boldsymbol{\Omega}_1 - x_1\boldsymbol{\Omega}_2)^2\right] + \frac{m_1}{2}\left[x_2^2\boldsymbol{\Omega}_3^2 + \dot{x}_2^2 + x_2^2\boldsymbol{\Omega}_1^2\right]. \tag{2}$$

Here m_2 is the mass of the proof mass and m_1 is the mass of the decoupling frame. Potential energy of the sensitive element is formed by stiffness of its springs and is given by the following formula:

$$E_P = \frac{k_1}{2}x_1^2 + \frac{k_2}{2}x_2^2, \tag{3}$$

where k_1 is the total stiffness of the elastic suspension along the axis X_1 and k_2 is the total stiffness along the axis X_2. Taking into consideration expressions for the kinetic energy (2), potential energy (3), substituting them into equations (1), the following system of two ordinary differential equations that describe motion of the sensitive element of the generalised single mass micro-mechanical gyroscope will appear after some simple transformations:

$$\begin{cases} \ddot{x}_1 + \left(\omega_{01}^2 - \Omega_2^2 - \Omega_3^2\right)x_1 + 2d\Omega_3\dot{x}_2 + d\left(\Omega_1\Omega_2 + \dot{\Omega}_3\right)x_2 = q_1, \\ \ddot{x}_2 + \left(\omega_{02}^2 - \Omega_1^2 - \Omega_3^2\right)x_2 - 2\Omega_3\dot{x}_1 + \left(\Omega_1\Omega_2 - \dot{\Omega}_3\right)x_1 = q_2, \end{cases} \tag{4}$$

where $\omega_{01}^2 = k_1/(m_1 + m_2)$ and $\omega_{02}^2 = k_2/m_2$ are natural frequencies of primary and secondary oscillations respectively, $d = m_2/(m_1 + m_2)$ is dimensionless inertia asymmetry factor, $q_1 = Q_1/(m_1 + m_2)$, $q_2 = Q_2/m_2$ are generalized accelerations caused by external forces, which act along respective axes. Note that if we simply assume that mass of the decoupling frame is zero ($m_1 = 0$) then $d = 1$ and we can obtain motion equations for the single mass micro-mechanical gyroscope without decoupling frame. Finally, equation

system (4) can be quite easily improved by introducing damping forces terms

$$\begin{cases} \ddot{x}_1 + 2\zeta_1\omega_{01}\dot{x}_1 + \left(\omega_{01}^2 - \Omega_2^2 - \Omega_3^2\right)x_1 + 2d\Omega_3\dot{x}_2 + d\left(\Omega_1\Omega_2 + \dot{\Omega}_3\right)x_2 = q_1, \\ \ddot{x}_2 + 2\zeta_2\omega_{02}\dot{x}_2 + \left(\omega_{02}^2 - \Omega_1^2 - \Omega_3^2\right)x_2 - 2\Omega_3\dot{x}_1 + \left(\Omega_1\Omega_2 - \dot{\Omega}_3\right)x_1 = q_2. \end{cases} \tag{5}$$

Here ζ_1 and ζ_2 are the dimensionless damping factors that correspond to the primary and secondary oscillations of the sensitive element.

It is apparent from analysis of the equations (5) that in case of ideal elastic suspension primary and secondary motion equations in this system are coupled only by means of the angular rate terms. It means that given absence of any external forces acting on the proof mass along generalized coordinate x_2 any forced displacements in this direction will be caused by the angular rate alone. Detailed consideration of the equation system (6) reveals that the angular rate is an unknown parameter of the system that makes the system (6) consisting of linear equations but with variable coefficients. Usually it is quite complicated task to find closed form analytical solution of such system in the general case.

Now let us move on to the consideration of the sensitive element with rotational both primary and secondary motions. Kinematical scheme will be the same as in the previous case except that generalised coordinates now represent angles rather than translational displacements. In this case α_1 corresponds to the angle between base and the decoupling frame, and α_2 corresponds to the angle between decoupling frame and the proof mass. Also all springs are rotational now. Needless to say that this case is slightly more complicated that the case of translational motion of the sensitive elements.

Components of the external angular rate vector $\vec{\Omega}$ given in the reference frame, which is assigned to the decoupling frame, are as follows:

$$\begin{aligned} \Omega_{11} &= \Omega_1 + \dot{\alpha}_1, \\ \Omega_{12} &= \Omega_2\cos\alpha_1 + \Omega_3\sin\alpha_1, \\ \Omega_{13} &= \Omega_2\sin\alpha_1 + \Omega_3\cos\alpha_1. \end{aligned} \tag{6}$$

Transforming them into the reference frame assigned to the proof mass results in the following expressions:

$$\begin{aligned} \Omega_{21} &= \Omega_{11}\cos\alpha_2 - \Omega_{13}\sin\alpha_2, \\ \Omega_{22} &= \Omega_{12} + \dot{\alpha}_2, \\ \Omega_{23} &= \Omega_{11}\sin\alpha_2 + \Omega_{13}\cos\alpha_2. \end{aligned} \tag{7}$$

With respect to the expressions (6) and (7), the total kinetic energy of the perfectly symmetric sensitive element is

$$E_K = \frac{1}{2}\left(I_{11}\Omega_{11}^2 + I_{12}\Omega_{12}^2 + I_{13}\Omega_{13}^2 + I_{21}\Omega_{21}^2 + I_{22}\Omega_{22}^2 + I_{23}\Omega_{23}^2\right). \tag{8}$$

Here I_{ij} are the moments of inertia of the i-th element (i = 1 – corresponds to the decoupling frame, i = 2 – corresponds to the proof mass) around j-th axis of the reference frame. Potential energy of the sensitive element is similar to the case of translational motions

$$E_P = \frac{k_1}{2}\alpha_1^2 + \frac{k_2}{2}\alpha_2^2, \tag{9}$$

where k_i are the angular spring constants of the elastic suspension. Given the expressions (8) and (9) for the kinetic and potential energies respectively, and again using Lagrange equations (1) we can obtain following motion equations

$$\begin{cases} \ddot{\alpha}_1 + 2\zeta_1\omega_{01}\dot{\alpha}_1 + \omega_{01}^2\alpha_1 + g_1\Omega_3\dot{\alpha}_2 - d_1\big(\Omega_2^2 - \Omega_3^2\big)\alpha_1 \\ + d_3\big(\Omega_1\Omega_2 - \dot{\Omega}_3\big)\alpha_2 - d_1\Omega_2\Omega_3 + \dot{\Omega}_1 = q_1\big(t\big), \\ \ddot{\alpha}_2 + 2\zeta_2\omega_{02}\dot{\alpha}_2 + \omega_{02}^2\alpha_2 - g_2\Omega_3\dot{\alpha}_1 - d_2\big(\Omega_1^2 - \Omega_3^2\big)\alpha_2 \\ - \big(\dot{\Omega}_3 - d_1\Omega_1\Omega_2\big)\alpha_1 + d_2\Omega_1\Omega_3 + \dot{\Omega}_2 = q_2(t). \end{cases} \tag{10}$$

Here q_1 and q_2 are generalised angular accelerations caused by external torques acting on the frame and the proof mass respectively, d_i and g_i are the dimensionless inertia parameters, meaning of which will be given later. All others parameters have the same meaning as in the case of translational motion of the sensitive element. Note that motion equations (10) were derived using certain simplifications: angles α_1 and α_2 are small so that $\sin\alpha_i \approx \alpha_i$ and $\cos\alpha_i \approx 1$, all non-linear terms with respect to these angles are assumed to be negligible.

Unless we are interested in study of the cross-sensitivity of the micromechanical gyroscopes we can further simplify motion equations assuming that the reference basis rotates with an angular rate, of which the vector is $\vec{\Omega} = \{0, 0, \Omega_3\}$. Therefore, analysing motion equations (5) and (10) one can see, that these two systems of equations can be easily combined into a single system regardless of what kind of motion is under consideration:

$$\begin{cases} \ddot{x}_1 + 2\zeta_1\omega_{01}\dot{x}_1 + \big(\omega_{01}^2 - d_1\Omega_3^2\big)x_1 + g_1\Omega_3\dot{x}_2 + d_3\dot{\Omega}_3x_2 = q_1\big(t\big), \\ \ddot{x}_2 + 2\zeta_2\omega_{02}\dot{x}_2 + \big(\omega_{02}^2 - d_2\Omega_3^2\big)x_2 - g_2\Omega_3\dot{x}_1 - \dot{\Omega}_3x_1 = q_2(t). \end{cases} \tag{11}$$

Here $q_i\,(t)$ represents either linear or angular accelerations that are caused by external forces or torques acting about corresponding axis, x_i represents either linear or angular displacements of the sensitive element. The dimensionless factors in equation (11) are explained in table 1. In table 1, all moments of inertia are presented in the form I_{ij} where the first index refers to the part of the sensitive element (1 is the frame, 2 is the proof mass) while the second index refers to the axis; m_2 is the mass of the proof mass and m_1 is the mass of the decoupling frame. One should note that, in case of sensitive element without an additional frame, $m_1 = 0$. All parameters of inertia presented in table 1 are subjected to the design process. Let us note that the rotational sensitive elements are more amenable to optimization. Furthermore, the dynamics of a sensitive element of micromechanical gyroscopes can be entirely described by a set of parameters as follows: ω_{01} and ω_{02} are the natural frequencies of primary and secondary oscillations; ζ_1 and ζ_2 are the relative damping factors; ω is the operating (excitation) frequency. Natural frequencies and damping factors

TABLE 1. Dimensionless inertia parameters

	Translational	Rotational
d_1	1	$(I_{12} + I_{23} - I_{12} - I_{22})/(I_{11} + I_{21})$
d_2	1	$(I_{23} - I_{21})/I_{22}$
d_3	$2m_2/(m_1 + m_2)$	$(I_{21} - I_{23})/(I_{11} + I_{21})$
g_1	$2m_2/(m_1 + m_2)$	$(I_{22} + I_{21} - I_{23})/(I_{11} + I_{21})$
g_2	2	$(I_{22} + I_{21} - I_{23})/I_{22}$

entirely determine the structural parameters of the sensitive element, such as mass, length of springs and vacuum level among others, for any achievable fabrication process. On the other hand, characteristics, such as measurement range, sensitivity, resolution, bias and bandwidth are the subject of sensitive element design process.

Primary Mode and Optimal Excitation

Sometimes it is more convenient to consider angular rate sensing by means of a vibratory gyroscope as an amplitude modulation. Indeed, output signal is a response of a simple oscillator forced by primary oscillations that are modulated by the external angular rate. In this case primary oscillations is a carrier. It becomes apparent after analysing of motion equations (11), where a first equation describes primary oscillations while second corresponds to the secondary. If there is no external rotation ($\Omega_3 = 0$) the motion equations become independent

$$\begin{cases} \ddot{x}_1 + 2\zeta_1\omega_{01}\dot{x}_1 + \omega_{01}^2 x_1 = q_{10}\sin(\omega t + \sigma), \\ \ddot{x}_2 + 2\zeta_2\omega_{02}\dot{x}_2 + \omega_{02}^2 x_2 = 0. \end{cases} \tag{12}$$

Here q_{10} is the amplitude of the excitation, ω is the excitation frequency, and σ is the excitation phase. Assuming zero initial conditions ($\dot{x}_1 = \dot{x}_2 = x_1 = x_2 = 0$) solutions for equations (12) are

$$\begin{aligned} x_1(t) &= \frac{q_{10}}{\sqrt{\left(\omega_{01}^2 - \omega^2\right)^2 + 4\omega_{01}^2\zeta_1^2\omega^2}}\sin(\omega t + \gamma), \\ x_2(t) &= 0. \end{aligned} \tag{13}$$

Phase γ of the primary oscillations is given by

$$\operatorname{tg}(\sigma - \gamma) = \frac{2\zeta_1\omega_{01}\omega}{\omega_{01}^2 - \omega^2}.$$

Apparently, in order to perform reliable measurements of the angular rate, the carrier must by highly stable in terms of amplitude and frequency and its amplitude must be as high as possible.

The most widely used in micromechanical gyroscopes with translational motion of the sensitive element method of excitations is by means of electrostatic interdigitated structure, which often is referenced as a comb-drive (see figure 4).

Here V_1 is the voltage applied to stator of the comb drive, V_0 is the constant bias voltage applied to the sensitive element, φ is the phase shift between voltage applied to the upper and the lower combs. The main purpose of such a drive is to produce a perfect harmonic force that will excite primary oscillations. Total force acting on the sensitive element can be determined as

$$F_x = \frac{(V_1(\tau + \varphi) - V_0)^2}{2}\frac{dC_1}{dx} + \frac{(V_1(\tau) - V_0)^2}{2}\frac{dC_2}{dx}, \tag{14}$$

where C_1 and C_2 are the capacitances of the upper and lower comb structures in figure 4 respectively, x is the displacement of the sensitive element along corresponding axis. In case of the symmetrical and linear comb drives ($C_1 = C_2 = C$, $dC/dx = const$) force

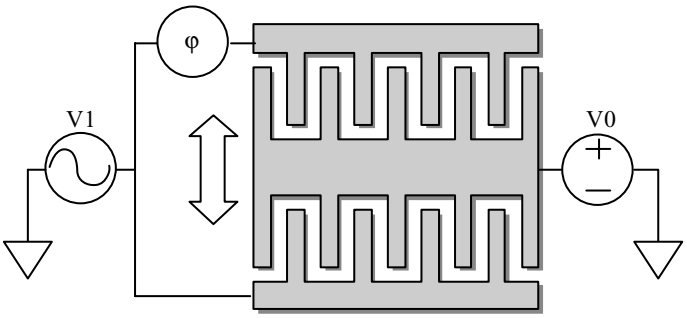

FIGURE 4. Excitation of the primary mode.

will be

$$F_x = \frac{1}{2}\left[(V_1(\tau+\varphi)-V_0)^2-(V_1(\tau)-V_0)^2\right]\frac{dC}{dx}.$$

If driving is harmonic we can assume that $V_1 = V\sin(\omega t)$, $V_0 = V\delta V$ and

$$F_x = \frac{V^2}{2}\left[(\sin(\omega t+\varphi)-\delta V)^2-(\sin(\omega t)-\delta V)^2\right]\frac{dC}{dx}. \tag{15}$$

One can see from formula (15) that the resulting force acting on the sensitive elements is far from being harmonic. Nevertheless, by proper tuning the phase shift φ we can significantly improve the situation. Let us determine the phase shift with respect to the maximum efficiency criterion. Assuming that the force does not depend on displacements, efficiency of the comb drive can be evaluated as follows:

$$P(\delta V,\varphi) = \int_0^{2\pi}\left[F(\tau)\right]^2 d\tau = \frac{\pi}{2}\left(1+8\delta V^2+\cos(\varphi)\right)\sin^2\left(\frac{\varphi}{2}\right)\frac{V^2}{2}\frac{dC}{dx}. \tag{16}$$

Graph of the efficiency (16) is shown in figure 5. It is apparent that there are two different optimal phase shifts as a function of δV.

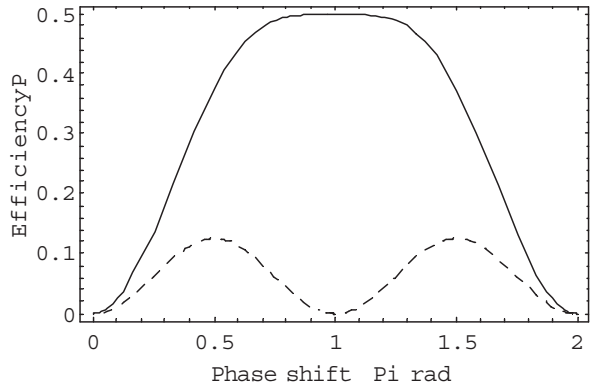

FIGURE 5. Efficiency of the excitation. (solid – $\delta V = 0.5$, dashed – $\delta V = 0$)

Maximum efficiency values for the phase shift φ and the voltage ratio δV as a parameter can be determined from the following equation

$$\frac{dP(\delta V, \varphi)}{d\varphi} = 0 \Rightarrow \left(4\delta V^2 + \cos\varphi\right)\sin\varphi = 0. \tag{17}$$

From (17) maximum efficiency phases are

$$\begin{aligned} \varphi = &\ \arccos\left(-4\delta V^2\right), \left(\delta V < \frac{1}{2}\right), \\ &\varphi = \pi, \left(\delta V \geq \frac{1}{2}\right), \\ &\varphi = \frac{\pi}{2}, (\delta V = 0). \end{aligned} \tag{18}$$

Thus there are two essential different driving modes of the sensitive element excitation: without bias voltage (grounded mass) and with bias, which is larger then a half of the driving voltage amplitude. Forces that acting on the mass in the such modes are given by the following formulae

$$\begin{aligned} F_x(t) &= V^2 \delta V \frac{dC}{dx}\sin(\omega t), \left(\delta V \geq \frac{1}{2}\right) - \text{“biased” mode}, \\ F_x(t) &= \frac{V^2}{4}\frac{dC}{dx}\cos(2\omega t), (\delta V = 0) - - \text{“grounded” mode}. \end{aligned} \tag{19}$$

It has to be noted that biased mode results in a larger driving force comparing with grounded mode (see figure 6).

However, driving force in the “grounded” mode will actuate with doubled frequency regarding to the driving voltage frequency.

Secondary Mode

Having looked at the primary oscillations of the sensitive element and methods of their efficient excitation, let us move on to the secondary oscillations. Studying solutions (13),

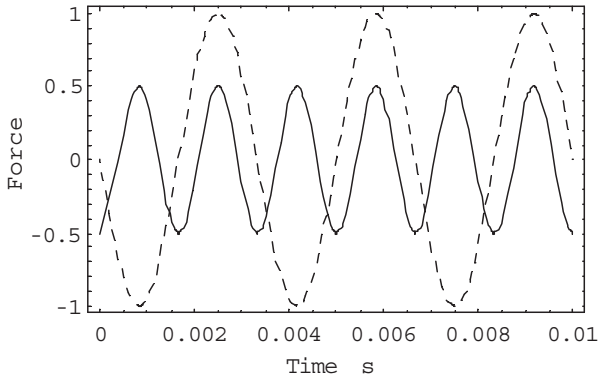

FIGURE 6. Excitation forces in different modes. (solid – grounded, dashed – biased)

one should see that if external angular rate is absent then secondary oscillations are absent as well. Now we assume that the external angular rate is present but is constant ($\dot{\Omega}_3 = 0$). Motion equations (11) become slightly simpler

$$\begin{cases} \ddot{x}_1 + 2\zeta_1\omega_{01}\dot{x}_1 + \left(\omega_{01}^2 - d_1\Omega_3^2\right)x_1 + g_1\Omega_3\dot{x}_2 = q_1(t), \\ \ddot{x}_2 + 2\zeta_2\omega_{02}\dot{x}_2 + \left(\omega_{02}^2 - d_2\Omega_3^2\right)x_2 - g_2\Omega_3\dot{x}_1 = q_2(t). \end{cases} \tag{20}$$

Assuming an open loop operation of the gyroscope and zero phase shift for the excitation force, we can represent the right-hand part of equations (20) as follows:

$$\begin{aligned} q_1(t) &= \operatorname{Re}\left\{q_1 e^{i\omega t}\right\}, \\ q_2(t) &= 0. \end{aligned} \tag{21}$$

We can also represent our generalized variables as it is accepted in the method of averaging

$$\begin{aligned} x_1(t) &= \operatorname{Re}\left\{\overline{A}_1 e^{i\omega t}\right\}, \overline{A}_1 = A_1 e^{i\varphi_1}, \\ x_2(t) &= \operatorname{Re}\left\{\overline{A}_2 e^{i\omega t}\right\}, \overline{A}_2 = A_2 e^{i\varphi_2}, \end{aligned} \tag{22}$$

where A_1 and A_2 are the amplitudes and φ_1 and φ_2 are the phases of the primary and secondary oscillations respectively. Using expressions (21) and (22), a complex solution of the equations (20) can be obtained:

$$\begin{aligned} \overline{A}_1 &= \frac{q_1\left(\omega_{02}^2 - d_2\Omega_3^2 - \omega^2 + 2\zeta_2\omega_{02}i\omega\right)}{\overline{\Delta}}, \\ \overline{A}_2 &= \frac{g_2 q_1 i\omega}{\overline{\Delta}}\Omega_3, \\ \overline{\Delta} &= \left(\omega_{01}^2 - d_1\Omega_3^2 - \omega^2\right)\left(\omega_{02}^2 - d_2\Omega_3^2 - \omega^2\right) \\ &\quad - \omega^2\left(4\zeta_1\zeta_2\omega_{01}\omega_{02} + g_1 g_2\Omega_3^2\right) \\ &\quad + 2i\omega\left[\omega_{01}\zeta_1\left(\omega_{02}^2 - d_2\Omega_3^2 - \omega^2\right)\right. \\ &\quad \left. + \omega_{02}\zeta_2\left(\omega_{01}^2 - d_1\Omega_3^2 - \omega^2\right)\right]. \end{aligned} \tag{23}$$

Keeping in mind expressions (22), real amplitudes of the primary and secondary oscillations can be obtained from expressions (23):

$$\begin{aligned} A_1 &= \frac{q_1\sqrt{\left(\omega_{02}^2 - d_2\Omega_3^2 - \omega^2\right)^2 + 4\omega_{02}^2\zeta_2^2\omega^2}}{\Delta_0}, \\ A_2 &= \frac{g_2 q_1\omega}{\Delta_0}\omega_3, \\ \Delta_0^2 &= \left[\left(\omega_{01}^2 - d_1\Omega_3^2 - \omega^2\right)\left(\omega_{02}^2 - d_2\Omega_3^2 - \omega^2\right)\right. \\ &\quad \left. - \omega^2\left(4\zeta_1\zeta_2\omega_{01}\omega_{02} + g_1 g_2\Omega_3^2\right)\right]^2 \\ &\quad + 4\omega^2\left[\omega_{01}\zeta_1\left(\omega_{02}^2 - d_2\Omega_3^2 - \omega^2\right)\right. \\ &\quad \left. + \omega_{02}\zeta_2\left(\omega_{01}^2 - d_1\Omega_3^2 - \omega^2\right)\right]^2. \end{aligned} \tag{24}$$

Note, that amplitude of the secondary oscillations is almost linearly related to the angular rate. Almost means that the angular rate is also present in denominator of the amplitude, which limits range of linearity for the sensor at high angular rates. Nevertheless, if one can detect this amplitude, some fairly good evaluations about external angular rate can be performed.

The real phases of the primary and secondary oscillations are given by the following expressions:

$$\begin{aligned}
\operatorname{tg}(\varphi_1) &= \frac{2\omega\left[\left(\omega_{02}^2 - d_2\Omega_3^2 - \omega^2\right)b_1 + \omega_{02}\zeta_2 b_2\right]}{\left(\omega_{02}^2 - d_2\Omega_3^2 - \omega^2\right)b_2 - 4\omega_{02}\zeta_2\omega^2 b_1}, \\
\operatorname{tg}(\varphi_2) &= \frac{\left(\omega_{01}^2 - d_1\Omega_3^2 - \omega^2\right)\left(\omega_{02}^2 - d_2\Omega_3^2 - \omega^2\right) - \omega^2\left(4\zeta_1\zeta_2\omega_{01}\omega_{02} + g_1 g_2\Omega_3^2\right)}{2\omega\left[\omega_{01}\zeta_1\left(\omega_{02}^2 - d_2\Omega_3^2 - \omega^2\right) + \omega_{02}\zeta_2\left(\omega_{01}^2 - d_1\Omega_3^2 - \omega^2\right)\right]}, \\
b_1 &= \omega_{01}\zeta_1\left(\omega_{02}^2 - d_2\Omega_3^2 - \omega^2\right) + \omega_{02}\zeta_2\left(\omega_{01}^2 - d_1\Omega_3^2 - \omega^2\right), \\
b_2 &= \left(\omega_{01}^2 - d_1\Omega_3^2 - \omega^2\right)\left(\omega_{02}^2 - d_2\Omega_3^2 - \omega^2\right) - \omega^2\left(4\zeta_1\zeta_2\omega_{01}\omega_{02} + g_1 g_2\Omega_3^2\right).
\end{aligned} \tag{25}$$

Using formulae (24) and (25) to obtain the amplitudes and phases respectively, we can now analyse sensitivity of a single mass micromechanical vibratory gyroscopes as well as its other important performances.

Scale Factor and Its Linearity

As follows from (24), the amplitude of secondary oscillations is related to the angular rate. Let us represent this amplitude by dimensionless variables by means of the following substitution:

$$\omega_{01} = \omega_0,\ \omega_{02} = \omega_0\delta\omega_0,\ \omega = \omega_0\delta\omega,\ \Omega_3 = \omega_0\delta\Omega. \tag{26}$$

As a function of new dimensionless variables amplitude of secondary oscillations is given by

$$\begin{aligned}
A_2 &= \frac{g_2 q_1 \delta\omega}{\omega_0^2\Delta}\delta\Omega, \\
\Delta^2 &= \left[\left(\delta\omega_0^2 - d_2\delta\Omega^2 - \delta\omega^2\right)\left(1 - d_1\delta\Omega^2 - \delta\omega^2\right)\right. \\
&\quad \left. - \delta\omega^2\left(4\delta\omega_0\zeta_1\zeta_2 + g_1 g_2\delta\Omega^2\right)\right]^2 \\
&\quad + 4\delta\omega^2\left[\delta\omega_0\zeta_2\left(1 - d_1\delta\Omega^2 - \delta\omega^2\right)\right. \\
&\quad \left. + \zeta_1\left(\delta\omega_0^2 - d_2\delta\Omega^2 - \delta\omega^2\right)\right]^2.
\end{aligned} \tag{27}$$

Graphic plot of the amplitude as a function of relative angular rate is shown in figure 7.

One should note that no assumption has been made about the value of the angular rate. It is obvious from figure 7 that the relationship between the secondary amplitude and the angular rate is not linear for high angular rates. However, in order to deliver acceptable performance of the gyroscope this dependence has to be linear. The scale factor can be taken as a tangent at the origin to the curve that is presented by dependence (27). In this

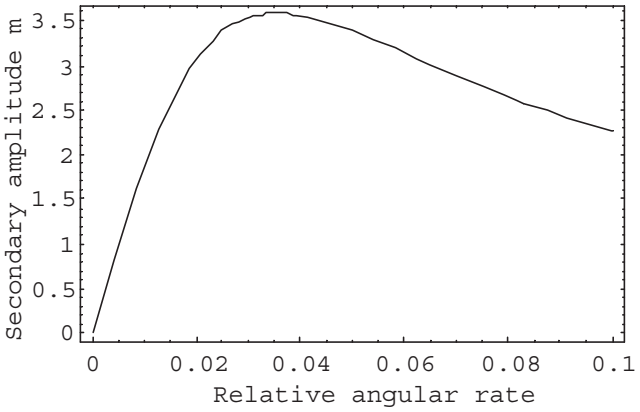

FIGURE 7. Amplitude of secondary oscillations. ($\omega_0 = 2000\pi$ s^{-1}, $\zeta_1 = \zeta_2 = 0.025$, $\delta\omega = 1$, $\delta\omega_0 = 1$)

case, scale factor for the relative angular rate $\delta\omega$ will be given by

$$C_\Omega = \frac{g_2 q_1 \delta\omega}{\omega_0^3 \sqrt{\left(\left(\delta\omega_0^2 - \delta\omega^2\right)^2 + 4\delta\omega_0^2\delta\omega^2\zeta_2^2\right)\left(\left(1 - \delta\omega^2\right)^2 + 4\delta\omega^2\zeta_1^2\right)}}, \tag{28}$$

where $A_{20} = C_\Omega\omega$ is the desirable output as compared with A_2. The dependence of the scale factor on the natural frequencies ratio $\delta\omega_0$ for different excitation frequencies $\delta\omega$ is shown in figure 8. Analysis of figure 8 shows that the greatest sensitivity is achievable only if natural frequencies are equal and excitation occurs on the eigenfrequency of primary oscillations. Moreover, considering (28) it is obvious that for better sensitivity the natural frequency of primary oscillations ω_0 has to be as low as possible. However, since sensitivity is not the only requirement for the angular rate sensor, exact matching of the natural frequencies usually is not the best choice. On the other hand, this leads us to the non-linear angular rate transformation.

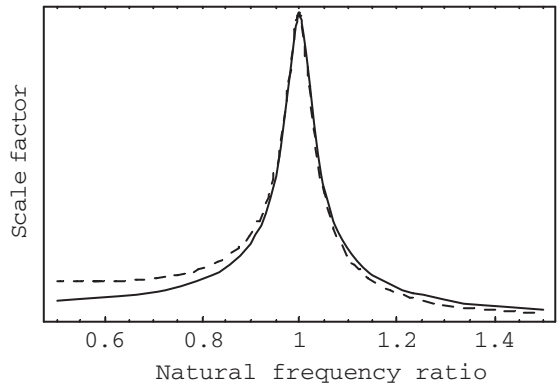

FIGURE 8. Scale factor as a function of natural frequency ratio $\delta\omega_0$. (solid – $\delta\omega = 1$, dashed - $\delta\omega = \delta\omega_0$)

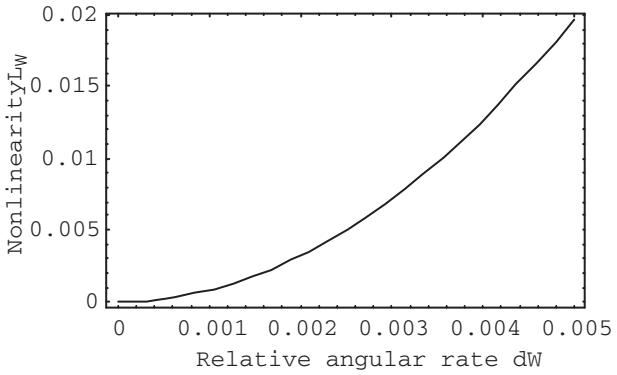

FIGURE 9. Nonlinearity as a function of the relative angular rate. ($\zeta_1 = \zeta_2 = 0.025$, $g_1 = 1$, $g_2 = 2$, $d_1 = 1$)

Let us introduce a non-linearity dimensionless factor as

$$L_\Omega = 1 - \frac{A_2}{A_{20}}.$$

The relationship between L_Ω and the angular rate $\delta\Omega$ is shown in figure 9.

For given small values of non-linearity L_Ω $(0 \ldots 0.05)$ we can obtain following the approximate formula for corresponding relative angular rate

$$\delta\Omega^* = \left\{ \frac{L_\Omega \left[\left(\delta\omega_0^2 - \delta\omega^2\right)^2 + 4\delta\omega_0^2\delta\omega^2\zeta_2^2 \right] \left[\left(1 - \delta\omega^2\right)^2 + 4\delta\omega^2\zeta_1^2 \right]}{\left(\delta\omega^2 - 1\right) D_0 + 4\delta\omega^2 \left[g_1 g_2 \delta\omega_0 \delta\omega^2 \zeta_1 \zeta_2 - d_2 \zeta_1^2 \left(\delta\omega_0^2 - \delta\omega^2\right) \right]} \right\}^{\frac{1}{2}}, \tag{29}$$

$$D_0 = \left(\delta\omega_0^2 - \delta\omega^2\right)\left(d_2 + d_1\delta\omega_0^2 - (d_2 + d_1 - g_1 g_2)\,\delta\omega^2\right) + 4d_1\delta\omega_0^2\delta\omega^2\zeta_2^2.$$

Assuming an acceptable value for the non-linearity L_ω and a required measurement range of the angular rate $\Omega_{\max}$, taking into consideration $\delta\Omega^*$ from expression (29) and substitutions (26), we can calculate the minimal acceptable value for the natural frequency of primary oscillations

$$\omega_{0\,\min} = \frac{\Omega_{\max}}{\delta\Omega^*}. \tag{30}$$

For example, if $L_\Omega = 0.01$ (1% scale factor nonlinearity) and $\Omega_{\max} = 1.0\,s^{-1}$ then the minimal value for the natural frequency of primary oscillations will be $\omega_0 \approx 45$ Hz. Such a low value for the frequency means that the lower limit could be determined in fact by other factors, but nevertheless there is no reason to make it higher than it is really necessary.

Resolution and dynamic range

There are many different ways for detecting displacements of the proof mass, such as capacitive, piezoresistive, piezoelectric, magnetic, optical, so far so forth. Needless to say that the simplest to implement and the most widely spread among micromechanical devices is, of course, capacitive. Assuming that one uses capacitive detection of the secondary oscillations, the formula for calculating the resolution of the micromechanical vibratory

gyroscope can be obtained be means of given minimal capacitance changes, which the system is capable of detecting. Let us denote this minimal change of capacitance as $\Delta C_{\min}$. Since capacitance C is a function of proof mass displacement δ, we can write

$$C(\delta) = C(0) + \frac{dC(0)}{d\delta}\delta + O(\delta^2).$$

For the small displacements, which is true for the secondary oscillations, we can neglect by $O(\delta^2)$ terms and the capacitance change will be given as

$$\Delta C(\delta) = C(\delta) - C(0) \approx \frac{dC(0)}{d\delta}\delta.$$

In case of differential measurement, which are quite commonly accepted in capacitance measurements, the resulting capacitance change is produced by subtraction of two separately measured capacitances C_1 and C_2 as follows:

$$\Delta C(\delta) = C_1(\delta) - C_2(\delta) \approx 2\frac{dC(0)}{d\delta}\delta. \tag{31}$$

For example, change in capacitance of two parallel conductive plates caused by displacements of the proof mass in case of differential measurement (31) can be calculated by the following formula

$$\Delta C = \frac{\varepsilon\varepsilon_0 S}{\delta_0 - \delta} - \frac{\varepsilon\varepsilon_0 S}{\delta_0 + \delta} \approx 2\frac{\varepsilon\varepsilon_0 S}{\delta_0^2}\delta.$$

Here, δ_0 is the base gap between the electrodes, δ is the displacement of the electrodes, S is the overlapped area, ε is the relative dielectric constant of the proof mass environment and ε_0 is the absolute dielectric constant of vacuum. The shift of the electrodes caused by changes of the angular rate $\Delta\Omega$ is given by

$$\delta = r_0 C_\Omega \Delta\Omega, \tag{32}$$

where C_Ω is determined by expression (28), r_0 is the distance from the rotation axis to the centre of electrode for the rotary sensitive element and unity for the translational sensitive element. Thus, comparing equations (31) and (32), we can obtain the resolution of a single mass micromechanical vibratory gyroscope that is given by

$$\Delta\Omega_{\min} = \frac{\Delta C_{\min}\omega_0^3\sqrt{\left(\left(\delta\omega_0^2 - \delta\omega^2\right)^2 + 4\delta\omega_0^2\delta\omega^2\zeta_2^2\right)\left(\left(1 - \delta\omega^2\right)^2 + 4\delta\omega^2\zeta_1^2\right)}}{2\dfrac{dC(0)}{d\delta}r_0 g_2 q_1 \delta\omega}. \tag{33}$$

Here the best resolution corresponds to a minimal $\Delta\Omega_{\min}$. Note that formula (33) represents the resolution with a capacitive differential readout. However, the same procedure can be applied to any readout principle using expression (28) for the scale factor. The resolution, which is given by formula (33), is related to the dynamics of the sensitive element and is fundamental from the design point of view. The real resolution of the gyroscope cannot be better than the one determined by the dynamics of its sensitive element. Unfortunately, the resolution can be worse since it is also affected by noise.

The resolution alone would never give to the user complete understanding of the measuring capabilities of a micromechanical gyroscope since it is tightly linked to the measurement

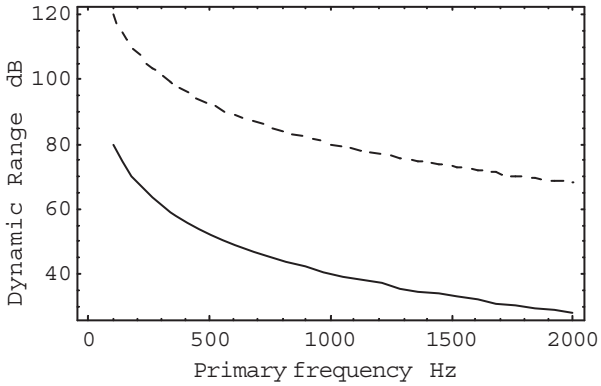

FIGURE 10. Dynamic range as a function of the primary natural frequency. (solid - $\zeta_1 = \zeta_2 = 0.025$, dashed – $\zeta_1 = \zeta_2 = 0.0025$, $\delta\omega = \delta\omega_0 = 1$)

range. The same resolution over different measurement ranges will correspond to the gyroscopes with entirely different performances. Therefore another characteristic is widely used to describe measuring capabilities of sensors, namely dynamic range, which in case of an angular rate sensor is defined as follows:

$$R = 20 \log_{10} \frac{\Omega_{\max} - \Delta\Omega_{\min}}{\Delta\Omega_{\min}}. \tag{34}$$

Here the dynamic range R is expressed in dB, $\Delta\Omega_{\min}$ is given by expression (33), assuming that the sensor threshold is equal to its resolution, $\Omega_{\max}$ is the maximum angular rate that can be measured with acceptable errors, which can be determined from expression (30):

$$\Omega_{\max} = \delta\Omega^* \omega_0, \tag{35}$$

where ω_0 is the natural frequency of the primary oscillations. Graphic plot of the dynamic range as a function of the primary natural frequency is shown in figure 10.

Looking at figure 10, one can see that the lower the primary natural frequency the higher will be dynamic range of the micromechanical vibratory gyroscope. Needless to say that for any reasonable required dynamic range the corresponding sensitive element can be designed even without vacuum packaging (solid line in figure 10). Despite this obvious fact, micromechanical vibratory gyroscopes are still referred to as a low-grade angular rate sensor. The reason for that is usage of micromachining for the fabrication of the gyroscopes in particular and the approach towards development of "miniature" sensors in general. As soon as designers try to develop a "micromechanical" gyroscope they make it extremely small in size, comparing to the conventional angular rate sensors. The overall size of the sensitive element in every direction varies from 100 micron to 5000 micron. As a result, the natural frequency of the primary oscillations ends up in a range from 5 kHz to 100 kHz. Apparently, in order to produce any, not mentioning high grade, angular rate sensing with such devices extremely high vacuum packaging is necessary. On the other hand, if one will try to design a gyroscope with low primary frequency, this will require making huge proof mass and very thin and long springs of the elastic suspension. This is quite complicated task if micromachining is used, especially considering very high relative tolerances of this fabrication process.

Bias

Bias in micromechanical gyroscopes can be the result of many different factors. Let us consider sources of bias concerned with the sensitive element and its dynamics. One of these is vibration at the excitation frequency. The interference of vibrations at other frequencies will be small and can be filtered. It is obvious, that for the translational gyroscopes, only translational vibration will have an effect, and for rotational gyroscopes only angular vibrations will be relevant. Therefore, in the case of vibrations at operation frequency, the motion equations of the sensitive element will be

$$\begin{cases} \ddot{x}_1 + 2\zeta_1\omega_{01}\dot{x}_1 + \left(\omega_{01}^2 - d_1\Omega_3^2\right)x_1 + g_1\Omega_3\dot{x}_2 = q_1(t) + w_1(t), \\ \ddot{x}_2 + 2\zeta_2\omega_{02}\dot{x}_2 + \left(\omega_{02}^2 - d_2\Omega_3^2\right)x_2 - g_2\Omega_3\dot{x}_1 = w_2(t). \end{cases} \tag{36}$$

Here $w_1(t)$ and $w_2(t)$ are components of the acceleration vector that represents the motion of the base reference system. By representing the vibrations as $w_i = w_{i0}\cos(\omega t)$, we can obtain the solution on the amplitude of secondary oscillations in dimensionless form

$$A_{W2} = \frac{g_2 q_1 \delta\omega\delta\Omega + \sqrt{w_{20}^2\left(1 - \delta\Omega^2 - \delta\omega^2\right)^2 + \delta\omega^2\left(2\zeta_1 w_{20} + g_2\delta\Omega w_{10}\right)^2}}{\omega_0^2\Delta}. \tag{37}$$

If we denote the amplitude without vibrations as A_{20}, which is given by (27), then the relative error caused by vibration at excitation frequency is given by

$$\delta A_W = \frac{A_{W2} - A_{20}}{A_{20}} = \frac{\sqrt{w_{20}^2\left(1 - d_1\delta\Omega^2 - \delta\omega^2\right)^2 + \delta\omega^2\left(2\zeta_1 w_{20} + g_2\delta\Omega w_{10}\right)^2}}{g_2 q_1 \delta\omega\delta\Omega}. \tag{38}$$

Let us note that the error arising from vibration does not depend on ratio between the natural frequencies but depends on the relative drive frequency. This dependency is shown in figure 11.

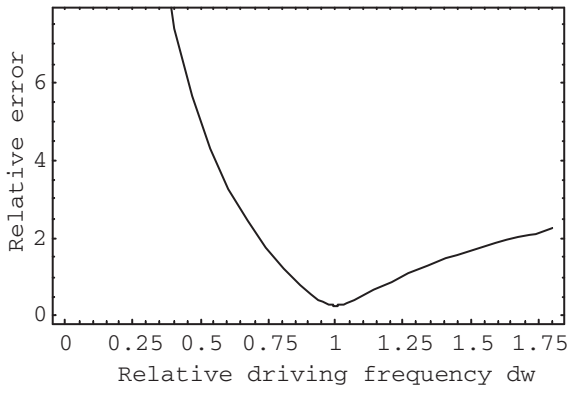

FIGURE 11. Typical error from vibrations as a function of relative driving frequency ($\zeta_1 = \zeta_2 = 0.025$, $g_1 = 1$, $g_2 = 2$, $d_1 = 1$, $q_1 = w_1 = w_2 = 1\text{m/s}^2$, $\delta\Omega = 10^{-4}$)

It can easily be proven that the minimal value for this error achievable at driving frequency is a solution of the following equation

$$1 - \delta\omega^2 - d_2\delta\Omega^2 = 0 \Rightarrow \delta\omega = \sqrt{1 - d_2\delta\Omega^2} \approx 1. \tag{39}$$

This result also ensures that it is preferable to drive the primary oscillations at their resonance.

Another source of bias is a misalignment between elastic and readout axes. This is most typical for the translation sensitive elements. The linearized motion equations in this case will be as follows

$$\begin{cases} \ddot{x}_1 + 2\zeta_1\omega_{01}\dot{x}_1 + \left(\omega_{01}^2 - d_1\Omega^2\right)x_1 + g_1\Omega\dot{x}_2 - 2\theta\Delta\omega_1^2 x_2 = q_1(t), \\ \ddot{x}_2 + 2\zeta_2\omega_{02}\dot{x}_2 + \left(\omega_{02}^2 - d_2\Omega^2\right)x_2 - g_2\Omega\dot{x}_1 + 2\theta\Delta\omega_2^2 x_1 = 0. \end{cases} \tag{40}$$

Here θ is the misalignment angle, $\Delta\omega_2^2 = (k_2 - k_1)/2M_2$, $\Delta\omega_1^2 = (k_1 - k_2)/2M_1$, where k_1 and k_2 are stiffness, corresponding to primary and secondary oscillations respectively, M_1 and M_2 are inertia factors that for translational motion $M_1 = m_1 + m_2$, $M_2 = m_2$, and for rotational motion $M_1 = I_{11} + I_{22}$, $M_2 = I_{22}$. The amplitude of the secondary oscillations in this case will be

$$\begin{aligned} A_2 &= \frac{q_1\sqrt{g_2^2\delta\omega^2\delta\Omega^2 + 4\theta^2\delta\Delta\omega_2^4}}{\omega_0^2\Delta_\theta}, \\ \Delta_\theta^2 &= \left[\left(\delta\omega_0^2 - d_2\delta\Omega^2 - \delta\omega^2\right)\left(1 - d_1\delta\Omega^2 - \delta\omega^2\right)\right. \\ &\quad - \left.\delta\omega^2\left(4\delta\omega_0\zeta_1\zeta_2 + g_1g_2\delta\Omega^2\right)\right]^2 \\ &\quad + 4\delta\omega^2\left[\delta\omega_0\zeta_2\left(1 - d_1\delta\Omega^2 - \delta\omega^2\right) + \zeta_1\left(\delta\omega_0^2 - d_2\delta\Omega^2 - \delta\omega^2\right)\right. \\ &\quad - \left.2\delta\Omega\theta\left(\delta\Delta\omega_1^2 + \delta\Delta\omega_2^2\right)\right]^2. \end{aligned} \tag{41}$$

It is apparent that if $\theta = 0$ then there is no error arising from misalignment. Moreover, this error will also be absent in the following case

$$\Delta\omega_2^2 = \frac{k_1 - k_2}{2m_2} = 0 \Rightarrow k_1 = k_2. \tag{42}$$

Here k_i are the stiffness factors of the elastic suspension and m_1 is the effective mass of secondary oscillations. In addition, we can represent the amplitude (42) as a sum of two components, namely, one arising from the angular rate and the other caused by misalignment

$$A_2 \approx A_{20} + A_{\theta 2}.$$

In this case we can determine the relative error from such misalignment as

$$\delta A_\theta = \frac{A_\theta}{A_{20}} = \frac{\theta^2\delta\Delta\omega_2^4}{g_2\delta\omega^2\delta\Omega^2}, (\Omega \neq 0). \tag{43}$$

On the other hand, we can find an acceptable tolerance for the misalignment $\theta_{\max}$ with respect to the given acceptable relative bias $\delta\Omega_{\max}$ and under the condition of no rotation

$$\theta_{\max} = \frac{\delta\Omega_{\max}\delta\omega}{\delta\Delta\omega_2^2}. \tag{44}$$

Formula (44) also gives us an angle of misalignment if bias is known. This value can be used for algorithmic bias compensation. If we can obtain information about external accelerations at the operation frequency the bias can be compensated based on dependence (38).

3. DYNAMIC ERROR AND BANDWIDTH

Even though we assumed earlier that the angular rate is constant the reality is not as simple as that. Nevertheless, every user of an angular rate sensor would like to be able to measure variable angular rates as good as constant ones at least to some certain extent. In order to represent variable angular rate it is assumed to have harmonic nature. Consequently, the range of angular rate frequencies in which sensor is able to measure angular rate with acceptable small error in amplitude, which is called dynamic error, and phase is referred to as a sensor bandwidth.

Let us consider movement of the sensitive element on a basis that rotates with harmonic angular rate

$$\Omega = \Omega_0 \cos(\lambda t) = \mathrm{Re}\left\{\omega_0 \mathrm{e}^{i\lambda t}\right\}.$$

Taking into account that the frequency of angular rate is small compared to the operation frequency, the corresponding motion equations of the sensitive element in this case are given by

$$\begin{cases} \ddot{x}_1 + 2\zeta_1\omega_{01}\dot{x}_1 + \left(\omega_{01}^2 - d_1\Omega^2\right)x_1 = q_1\cos(\omega t) - g_1\Omega\dot{x}_2 - d_3\dot{\Omega}x_2, \\ \ddot{x}_2 + 2\zeta_2\omega_{02}\dot{x}_2 + \left(\omega_{02}^2 - d_2\Omega^2\right)x_2 = g_2\Omega\dot{x}_1 + \dot{\Omega}x_1. \end{cases} \tag{45}$$

When the amplitude of the angular rate is small ($\Omega_0 \ll \omega_{01}$) and frequency λ of the harmonic angular rate is small in comparison with the natural frequency ω_{01}, we can neglect the right-hand terms in the first equation of system (45) except for the excitation term. In addition, centrifugal accelerations in this case are small and hence the equations reduce to

$$\begin{cases} \ddot{x}_1 + 2\zeta_1\omega_{01}\dot{x}_1 + \omega_{01}^2 x_1 = q_1\cos(\omega t), \\ \ddot{x}_2 + 2\zeta_2\omega_{02}\dot{x}_2 + \omega_{02}^2 x_2 = g_2\Omega\dot{x}_1 + \dot{\Omega}x_1. \end{cases} \tag{46}$$

The partial solution of the first equation of system (46) is given by the following:

$$x_1(t) = \mathrm{Re}\left\{\overline{A}_1\mathrm{e}^{i\omega t}\right\} = \mathrm{Re}\left\{A_1\mathrm{e}^{i(\omega t+\varphi_1)}\right\},$$

$$A_1 = \frac{q_1}{\omega_0^2\sqrt{\left(1-\delta\omega^2\right)^2 + 4\zeta_1^2\delta\omega^2}}, \quad \mathrm{tg}(\varphi_1) = -\frac{2\zeta_1\delta\omega}{1-\delta\omega^2}.$$

Then the right-hand part of the second equation in system (46) will be

$$-\frac{\Omega_0}{2}\mathrm{Im}\left\{\overline{A}_1(g_2\omega+\lambda)\mathrm{e}^{if_1 t} + \overline{A}_1(g_2\omega-\lambda)\mathrm{e}^{if_2 t}\right\}, \; f_{1,2} = \omega \pm \lambda.$$

The partial solution of non-homogeneous equation (46) for the secondary oscillations x_2 yields a solution given by a sum of two oscillations with frequencies $f_{1,2} = \omega \pm \lambda$

$$x_2(t) = \mathrm{Im}\left\{\overline{A}_{21}\mathrm{e}^{if_1 t} + \overline{A}_{22}\mathrm{e}^{if_2 t}\right\}.$$

After substitution of the supposed solution in the first equation of system (46) we can find complex amplitudes of secondary oscillations

$$\overline{A}_{21,22} = -\frac{\Omega_0 q_1 (g_2\delta\omega \pm \delta\lambda)}{2\omega_0^3\left[\delta\omega_0^2 - (\delta\omega \pm \delta\lambda)^2 + 2\zeta_2\delta\omega_0 i\,(\delta\omega \pm \delta\lambda)\right]\left[1 - \delta\omega^2 + 2\zeta_1 i\delta\omega\right]},$$

where $\delta\lambda = \lambda/\omega_0$ is the relative frequency of the angular rate. Transition to real amplitude and phase gives us

$$A_{21,22} = \frac{\omega_0 q_1 (g_2\delta\omega \pm \delta\lambda)}{2\omega_0^3\sqrt{\left\{\left[\delta\omega_0^2 - (\delta\omega \pm \delta\lambda)^2\right]^2 + 4\zeta_2^2\delta\omega_0^2(\delta\omega \pm \delta\lambda)^2\right\}\left\{(1-\delta\omega^2)^2 + 4\zeta_1^2\delta\omega^2\right\}}}.$$

Hence partial solution for the secondary oscillations is given by

$$x_2(t) = A_{21}\sin\left[(\omega + \lambda)t + \varphi_{21}\right] + A_{22}\sin\left[(\omega - \lambda)t + \varphi_{22}\right]. \tag{47}$$

Here the phase shifts $\varphi_{21,22}$ are determined from the following expression

$$tg(\varphi_{21}) = 2\frac{\delta\omega\zeta_1\left(\delta\omega_0^2 - (\delta\lambda + \delta\omega)^2\right) + \delta\omega_0\zeta_2\left(1 - \delta\omega^2\right)(\delta\omega + \delta\lambda)}{4\delta\omega_0\delta\omega\zeta_1\zeta_2(\delta\lambda + \delta\omega) - \left(1 - \delta\omega^2\right)\left(\delta\omega_0^2 - (\delta\omega + \delta\lambda)^2\right)},$$

$$tg(\varphi_{22}) = 2\frac{\delta\omega\zeta_1\left(\delta\omega_0^2 - (\delta\omega - \delta\lambda)^2\right) + \delta\omega_0\zeta_2\left(1 - \delta\omega^2\right)(\delta\omega - \delta\lambda)}{4\delta\omega_0\delta\omega\zeta_1\zeta_2(\delta\omega - \delta\lambda) - \left(1 - \delta\omega^2\right)\left(\delta\omega_0^2 - (\delta\omega - \delta\lambda)^2\right)}.$$

Assuming that $\omega = const \Rightarrow \delta\lambda = 0$, we can obtain the amplitude and phase of the secondary oscillations when the angular rate is constant. By making the following substitutions

$$A_{21,22} = A_{20}(1 \pm \delta A),\ \varphi_{11,12} = \varphi_0 \pm \Delta\varphi,$$

solution (47) will be changed to

$$x_2(t) = 2A_{20}\left[\cos(\lambda t + \Delta\varphi)\sin(\omega t + \varphi_0) + \delta A\sin(\lambda t + \Delta\varphi)\cos(\omega t + \varphi_0)\right].$$

After multiplying the signal corresponding to the secondary oscillations on a phase shifted carrier signal $\sin(\omega t + \varphi_0)$, the output will be as follows

$$\begin{aligned} x_2^*(t) = A_{20}[&\cos(\lambda t + \Delta\varphi) - \cos(\lambda t + \Delta\varphi)\cos(2\omega t + 2\varphi_0) \\ &+ \delta A\sin(\lambda t + \Delta\varphi)\sin(2\omega t + 2\varphi_0)]. \end{aligned}$$

The first item $A_{20}\cos(\lambda t + \Delta\varphi)$ is the signal related to the angular rate. All other items have doubled frequency and must to be removed by means of filtering after demodulation. Note that the output signal is distorted both in amplitude and phase. Phase distortion $\Delta\varphi$ is well predictable in a very wide range by means of obtained formulae. Amplitude error caused by the harmonic angular rate is determined as

$$\delta\Omega = \frac{A_{20} - A_0}{A_0} \approx D_\lambda\delta\lambda^2, \tag{48}$$

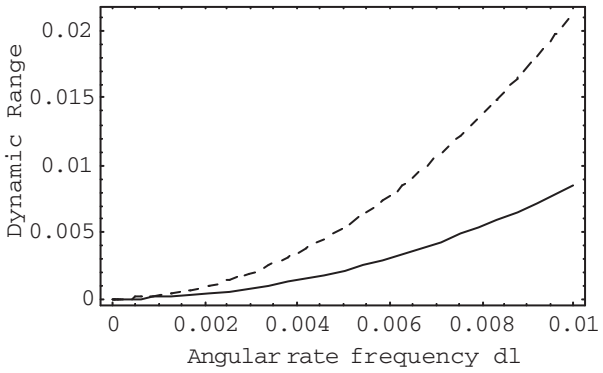

FIGURE 12. Dynamic error as a function of relative angular rate frequency. (dashed line $\delta\omega = 1.05$, solid line $\delta\omega = 1.1$, $\zeta_1 = \zeta_2 = 0.025$, $g_1 = 1$, $g_2 = 2$, $d_1 = d_2 = 1$, $q_1 = 10\,\mathrm{m/s^2}$, $\delta\omega_0 = 1$)

where

$$D_\lambda = \frac{\delta\omega^6 (3g_2 - 2) + h\delta\omega_0^2 \left[\delta\omega_0^4 (2 + g_2) - \delta\omega^4 (5g_2 - 6)\right] + \delta\omega_0^4 \delta\omega^2 \left[4h^2 (g_2 - 1) - 2 - 3g_2\right]}{g_2 \left[\left(\delta\omega_0^4 + \delta\omega^4 - 2\delta\omega_0^2 \delta\omega^2 h\right)\right]^2},$$

$$h = 1 - 2\zeta_2^2,\ A_0 = A_{20}\,(\delta\lambda = 0)\,.$$

Formula (48) gives only approximate results but for small values of the relative frequency of the angular rate ($\delta\lambda = 0...0.01$) they are acceptable. The exact formula is more complicated and there is no reason to use it in this context. Graphs corresponding to both approximate and exact dependences are shown in figure 12 but there is no visually detectable difference between them in the given range.

It is apparent that the dynamic error increases if the ratio between the natural frequencies approaches unity. In addition, it is possible to calculate a bandwidth if assume acceptable relative dynamic error $\delta\Omega_{\max}$

$$B_\Omega = \omega_0 \sqrt{\frac{\delta\Omega_{\max}}{D_\lambda}}. \tag{49}$$

Here bandwidth B_Ω is measured in radians per second. The graph for the relative bandwidth (B_Ω / ω_0) is shown in figure 13.

Analyzing both figures 13 and 8, we can see that, as the ratio of the natural frequencies approaches unity (i.e. $\delta\omega_0 \approx 1$), we obtain the maximal sensitivity but the minimal bandwidth. This effectively leads to a trade-off between these parameters. For open-loop gyroscopes, it is acceptable to have a ratio of the natural frequencies in the range of 0.9–0.95. For the closed-loop operation, it is reasonable to have a ratio $\delta\omega_0 \approx 1$ for maximal sensitivity while providing required bandwidth by the feedback.

Due to inaccuracies of the present fabrication technologies, springs and other elements of the elastic suspension may have unknown and unpredictable deviations from the design values. This will result in deviations in the main parameters of the sensitive element. As shown above, one of the main parameters which is important for both sensitivity and

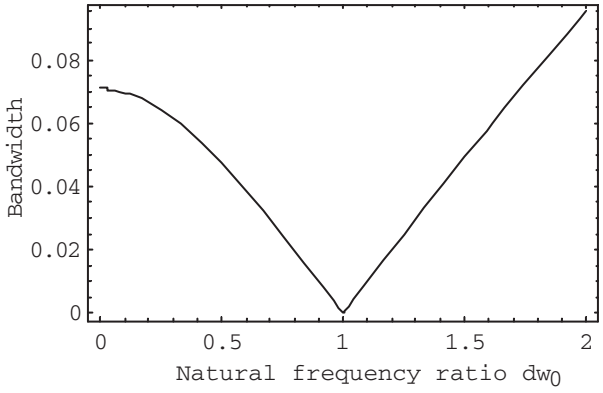

FIGURE 13. Relative bandwidth as a function of ratio of the natural frequencies. ($\delta\Omega_{\max} = 0.01$, $\zeta_1 = \zeta_2 = 0.0001$, $g_1 = 1$, $g_2 = 2$, $d_1 = d_2 = 1$, $q_1 = 10\,\mathrm{m/s^2}$, $\delta\omega_0 = 1$).

bandwidth is the ratio of the natural frequencies. Let us consider small deviations of natural frequencies caused by the production inaccuracies. Deviations of natural frequencies will result in the deviation of the ratio of the natural frequencies as given by

$$\delta\omega_0^* = \delta\omega_0\,(1 + \varepsilon_{\delta\omega})\,. \tag{50}$$

Using expression (50), we can calculate the relative deviation of the bandwidth that can be represented as follows

$$\delta B_\Omega = (B_\Omega - B_{\Omega 0})\big/ B_{\Omega 0}, \tag{51}$$

where $B_{\Omega 0}$ is the bandwidth corresponding to the absence of deviations ($\varepsilon_{\delta k} = 0$). For small deviations $\varepsilon_{\delta k}$, we can represent (51) by the following formula

$$\delta B_\Omega \approx \frac{D_{\varepsilon 1}}{D_{\varepsilon 2}}\varepsilon_{\delta\omega}, \tag{52}$$

where

$$\begin{aligned}
D_{\varepsilon 1} = {} & \delta\omega_0^2 \left\{ \left(\delta\omega^2 - \delta\omega_0^2\right)^3 \left[(g_2 + 2)\,\delta\omega_0^2 + (7g_2 - 2)\,\delta\omega^2\right] \right. \\
& - 8\delta\omega_0^2\delta\omega^2\zeta_2^4 \left[(5g_2 - 2)\,\delta\omega_0^4 + (g_2 - 2)\,\delta\omega^2\right] \\
& + 2\left(\delta\omega_0^2 - \delta\omega^2\right)\zeta_2^2 \left[(g_2 + 2)\,\delta\omega_0^6 + 3\,(7g_2 - 2)\,\delta\omega_0^4\delta\omega^2\right. \\
& \left. \left. + 3\,(2 + g_2)\,\delta\omega_0^2\delta\omega^4 + (7g_2 - 2)\,\delta\omega^6\right]\right\}, \\
D_{\varepsilon 2} = {} & \left[\left(\delta\omega_0^2 - \delta\omega^2\right)^2 + 4\delta\omega_0^2\delta\omega^2\zeta_2^2\right]\left\{(2 - 3g_2)\,\delta\omega^6\right. \\
& + (5g_2 - 6)\,h\delta\omega_0^2\delta\omega^4 + (2 + g_2)\,\delta\omega_0^6 h \\
& \left. + \delta\omega_0^4\delta\omega^2\left[6 - g_2 + 16\,(g_2 - 1)\,\zeta_2^2 - 16\,(g_2 - 1)\,\zeta_2^4\right]\right\}.
\end{aligned}$$

Note that this relative deviation of the bandwidth does not depend on the absolute value of the driving frequency.

4. DESIGN METHODOLOGY

The presented above analysis of the sensitivity, linearity and bandwidth have resulted in two design trade-offs. Firstly, in order to increase sensitivity, working frequency has to be as low as possible, but in the same time there is a lower limit that depends on scale factor linearity requirements. As a result, natural frequency of the primary oscillations can be chosen by means of formula (30) taking into consideration acceptable value of the non-linearity and required measurement range. Secondly, in order to obtain maximum sensitivity, both natural frequencies of primary and secondary oscillations have to be of the same value, but it will result in a minimum for the bandwidth. This trade-off can be resolved by formula (49) so the ratio of the natural frequencies will have to be designed providing necessary bandwidth. As a result, parameters such as driving frequency, primary frequency (natural frequency of the primary oscillations) and ratio of the natural frequencies can be directly calculated and they have to be precisely implemented during sensitive element design or feedback control loops design.

5. RESUME

The presented analytical approach to the design of the sensitive element of micromechanical vibratory gyroscopes allows both prediction of the performances and determination of the dynamic parameters that are necessary to achieve high performance of inertial instruments. Even though the proposed approach is applied to sensitive elements, most of the dependencies can also be used for detailed analysis of the dynamics of micromechanical gyroscopes while designing control circuits.

REFERENCES

1. Friedland, B. and Hutton, M.F., Theory and Error Analysis of Vibrating-Member Gyroscope, *IEEE Transactions on Automatic Control*, 1978;23:545–556.
2. Lynch, D., Vibratory Gyro Analysis by the Method of Averaging, *Proc. 2nd St. Petersburg Conf. on Gyroscopic Technology and Navigation (St. Petersburg)*, 1995, pp. 26–34.
3. Apostolyuk, V. and Zbrutsky, A., Research of Dynamics of a Gimballed Micromechanical Gyroscope, *Scientific news of the National Technical, University of Ukraine (Kiev)*, 1998, no. 3, pp. 115–121.
4. Apostolyuk, V. and Zbrutsky, A., Dynamics of a Sensitive Element of the Micromechanical Gyroscopes with an Additional Frame, *Gyroscopes and Navigation (St. Petersburg)*, 1998, Vol. 3(22), pp. 13–23.
5. Apostolyuk, V. and Zbrutsky, A., Dynamics of a Sensitive Element of Micromechanical Gyroscope, *Scientific news of the National Technical University of Ukraine (Kiev)*, 1999, no. 1, pp. 114–120.
6. Apostolyuk, V., Logeeswaran, V.J., and Tay, F., Efficient Design of Micromechanical Gyroscopes, *Journal of Micromechanics and Microengineering*, 2002, no. 12, pp. 948–954.